eral minutes to obtain near-field fluorescence spectra with good signal-to-noise ratios. Furthermore, the recent work of Xie and Dunn (*33*) and by Ambrose *et al.* (*34*) showed that the metal-coated probe tip can significantly perturb the electronic properties of the molecule being detected. In contrast, the far-field confocal fluorescence approach provides unlimited laser throughput and a three-dimensional sectioning capability and is truly noninvasive, although its resolution is diffraction limited. These features are expected to allow important applications such as enhanced Raman spectroscopy at the single-molecule level and on-line fluorescence identification and sorting of individual molecules and quantum-confined nanostructures. The extraordinary sensitivity achieved in this work allows the direct, real-time study of the dynamics of a single molecule and the chemical and biochemical reactions that such a molecule may undergo in solution.

REFERENCES AND NOTES

1. W. E. Moerner, *Science* **265**, 46 (1994), and references therein.
2. M. Orrit, J. Bernard, R. I. Personov, *J. Phys. Chem.* **97**, 10256 (1993).
3. F. Güttler, T. Irngartinger, T. Plakhotnik, A. Renn, U. P. Wild, *Chem. Phys. Lett.* **217**, 393 (1994).
4. M. Ishikawa, K. Hirano, T. Hayakawa, S. Hosoi, S. Brenner, *Jpn. J. Appl. Phys.* **33**, 1571 (1994).
5. E. Betzig and R. J. Chichester, *Science* **262**, 1422 (1993).
6. J. K. Trautman, J. J. Macklin, L. E. Brus, E. Betzig, *Nature* **369**, 40 (1994).
7. D. C. Nguyen, R. A. Keller, J. H. Jett, J. C. Martin, *Anal. Chem.* **59**, 2158 (1987).
8. K. Peck, L. Stryer, A. N. Glazer, R. A. Mathies, *Proc. Natl. Acad. Sci. U.S.A.* **86**, 4087 (1989).
9. W. B. Whitten, L. M. Ramsey, S. A. Arnold, B. V. Bronk, *Anal. Chem.* **63**, 1027 (1991); K. C. Ng, W. B. Whitten, S. A. Arnold, L. M. Ramsey, *ibid.* **64**, 2914 (1992).
10. M. Eigen and R. Rigler, *Proc. Natl. Acad. Sci. U.S.A.* **91**, 5740 (1994).
11. In fluorescence correlation spectroscopy, the intensity recorded at time t is multiplied by that recorded at $t + \Delta t$, and the product is integrated over a finite period of time; see D. E. Koppel, *Phys. Rev. A* **10**, 1938 (1974).
12. T. T. Perkins, D. E. Smith, S. Chu, *Science* **264**, 819 (1994); T. T. Perkins, S. R. Quake, D. E. Smith, S. Chu, *ibid.*, p. 822.
13. S. B. Smith, L. Finzi, C. Bustamante, *ibid.* **258**, 1122 (1992); C. Bustamante, *Annu. Rev. Biophys. Biophys. Chem.* **20**, 415 (1991).
14. M. Washizu and O. Kurosawa, *IEEE Trans. Ind. Appl.* **26**, 1165 (1990).
15. S. B. Smith, P. K. Aldridge, J. B. Callis, *Science* **243**, 203 (1989).
16. N. J. Rampino and A. Chrambach, *Anal. Biochem.* **194**, 278 (1991).
17. K. Morikawa and M. Yanagida, *J. Biochem.* **89**, 693 (1981).
18. I. Auzanneau, C. Barreau, L. Salome, *C. R. Acad. Sci. Paris* **316**, 459 (1993).
19. H. Kabata *et al.*, *Science* **262**, 1561 (1993).
20. D. A. Schafer, J. Gelles, M. P. Sheetz, R. Landick, *Nature* **352**, 444 (1991).
21. Laser excitation at 488.0 and 514.5 nm was provided by an argon ion laser (Lexel Lasers, Fremont, CA). The laser beam entered the microscope through a back port and was directed to an oil-immersion objective (×100, NA = 1.3, Nikon Instrument Group, Melville, NY) by a dichroic beamsplitter (505DRLP02 or 540DRLP02, Omega Optical Inc., Brattleboro, VT). The laser beam was focused to a diffraction-limited spot by the high NA objective in our study, which was verified qualitatively by comparing the laser focal size and 1-μm polystyrene microspheres (Duke Scientific, Palo Alto, CA). Fluorescence was collected by the same objective, passed the same dichroic beamsplitter, and was then directed to a side port by a reflective mirror. Efficient rejection of out-of-focus signals was achieved by placing a pinhole (50 to 100 μm diameter, Newport Corp., Irvine, CA) in the primary image plane. A single interference bandpass filter (Omega Optical Inc., Brattleboro, VT) was used to reject the laser light and the Rayleigh and Raman scattered photons. The fluorescence signal was then focused on a photon-counting Si avalanche photodiode (quantum efficiency, 55% at 630 nm, and dark noise, 7 counts per second) (Model SPCM-200, EG&G Canada, Vaudreuil, Quebec). Time-dependent data were acquired by using a multichannel scalar (EG&G ORTEC, Oak Ridge, TN) run on a personal computer (IBM PC-AT). Fluorescent dyes and other materials were purchased from Molecular Probes, Inc. (Eugene, OR), Eastman Chemicals (Kingsport, TN), and Sigma Chemical Corp. (St. Louis, MO).
22. M. B. Schneider and W. W. Webb, *Appl. Opt.* **20**, 1382 (1981).
23. R. Rigler, U. Mets, J. Widengren, P. Kask, *Eur. Biophys. J.* **22**, 169 (1993).
24. W. Feller, *An Introduction to Probability Theory and its Applications* (Wiley, New York, ed. 3, 1968).
25. S. A. Soper, H. L. Nutter, R. A. Keller, L. M. Davis, E. B. Shera, *Photochem. Photobiol.* **57**, 972 (1993).
26. A complicating factor is photobleaching, which converts the molecule being detected into a nonfluorescent state and prevents its further detection. The multiple detection and similar fluorescence intensity observed for molecules of greatly different photodestruction efficiencies (that is, R6G and fluorescein) indicate however that photobleaching is not significant in this study.
27. This calculation is based on the diffusion equation $\tau_D = \omega^2/2D$, where τ_D is the diffusion time, ω is the diffusion distance in one dimension, and D is the diffusion coefficient (2.8×10^{-6} cm^2 s^{-1} for rhodamine 6G in water/ethanol).
28. D. Magde, E. L. Elson, W. W. Webb, *Biopolymers* **13**, 1 (1974); *ibid.*, p. 29.
29. D. N. Dempster, T. Morrow, M. F. Quinn, *J. Photochem.* **2**, 343 (1973).
30. M. M. Asimov, V. N. Gavrilenko, A. N. Rubinov, *J. Lumin.* **46**, 243 (1990).
31. H. Qian and E. L. Elson, *Appl. Opt.* **30**, 1185 (1991).
32. E. Betzig, J. K. Trautman, T. D. Harris, J. S. Weiner, R. L. Kostelak, *Science* **251**, 1468 (1991); E. Betzig and J. K. Trautman, *ibid.* **257**, 189 (1992).
33. X. S. Xie and R. C. Dunn, *ibid.* **265**, 361 (1994).
34. W. P. Ambrose, P. M. Goodwin, J. C. Martin, R. A. Keller, *ibid.*, p. 364.
35. S.N. acknowledges the Whitaker Foundation for a young investigator award. D.T.C. is a Beckman Cell Science Scholar of Stanford University. This work was supported by Beckman Instruments, Inc.

18 July 1994; accepted 19 September 1994

Molecular Computation of Solutions to Combinatorial Problems

Leonard M. Adleman

The tools of molecular biology were used to solve an instance of the directed Hamiltonian path problem. A small graph was encoded in molecules of DNA, and the "operations" of the computation were performed with standard protocols and enzymes. This experiment demonstrates the feasibility of carrying out computations at the molecular level.

In 1959, Richard Feynman gave a visionary talk describing the possibility of building computers that were "sub-microscopic" (*1*). Despite remarkable progress in computer miniaturization, this goal has yet to be achieved. Here, the possibility of computing directly with molecules is explored.

A directed graph G with designated vertices v_{in} and v_{out} is said to have a Hamiltonian path (*2*) if and only if there exists a sequence of compatible "one-way" edges $e_1, e_2, \ldots, e_z$ (that is, a path) that begins at v_{in}, ends at v_{out}, and enters every other vertex exactly once. Figure 1 shows a graph that for $v_{in} = 0$ and $v_{out} = 6$ has a Hamiltonian path, given by the edges 0→1, 1→2, 2→3, 3→4, 4→5, 5→6. If the edge 2→3 were removed from the graph, then the resulting graph with the same designated vertices would not have a Hamiltonian path. Similarly, if the designated vertices were changed to $v_{in} = 3$ and $v_{out} = 5$ there would be no Hamiltonian path (because, for example, there are no edges entering vertex 0).

There are well-known algorithms for deciding whether an arbitrary directed graph with designated vertices has a Hamiltonian path or not. However, all known algorithms for this problem have exponential worst-case complexity, and hence there are instances of modest size for which these algorithms require an impractical amount of computer time to render a decision. Because the directed Hamiltonian path problem has been proven to be NP-complete, it seems likely that no efficient (that is, polynomial time) algorithm exists for solving it (*2*, *3*).

The following (nondeterministic) algorithm solves the directed Hamiltonian path problem:

Step 1: Generate random paths through the graph.

Step 2: Keep only those paths that begin with v_{in} and end with v_{out}.

Step 3: If the graph has n vertices, then keep only those paths that enter exactly n vertices.

Step 4: Keep only those paths that enter all of

Department of Computer Science and Institute for Molecular Medicine and Technology, University of Southern California, 941 West 37th Place, Los Angeles, CA 90089, USA.

the vertices of the graph at least once.

Step 5: If any paths remain, say "Yes"; otherwise, say "No."

The graph shown in Fig. 1 with designated vertices $v_{in} = 0$ and $v_{out} = 6$ was solved with the algorithm above implemented at the molecular level. Note that the labeling of the vertices in such a way that the (unique) Hamiltonian path enters the vertices in sequential order is only for convenience in this exposition and provides no advantage in the computation. The graph is small enough that the Hamiltonian path can be found by visual inspection; however, it is large enough to demonstrate the feasibility of this approach. It seems clear that the methods described here could be scaled-up to accommodate much larger graphs.

To implement Step 1 of the algorithm, each vertex i in the graph was associated with a random 20-mer sequence of DNA denoted O_i. For each edge $i \rightarrow j$ in the graph, an oligonucleotide $O_{i \rightarrow j}$ was created that was the 3′ 10-mer of O_i (unless $i = 0$, in which case it was all of O_i) followed by the 5′ 10-mer of O_j (unless $j = 6$, in which case it was all of O_j). Notice that this construction preserves edge orientation. For example, $O_{2 \rightarrow 3}$ will not be the same as $O_{3 \rightarrow 2}$. The 20-mer oligonucleotide with the sequence that is Watson-Crick complementary to O_i was denoted $\overline{O}_i$ (Fig. 2).

For each vertex i in the graph (except $i = 0$ and $i = 6$) and for each edge $i \rightarrow j$ in the graph, 50 pmol of $\overline{O}_i$ and 50 pmol of $O_{i \rightarrow j}$, respectively, were mixed together in a single ligation reaction (4). The $\overline{O}_i$ oligonucleotides served as splints to bring oligonucleotides associated with compatible edges together for ligation (Fig. 2). Hence the ligation reaction resulted in the formation of DNA molecules encoding random paths through the graph.

The scale of this ligation reaction far exceeded what was necessary for the graph under consideration. For each edge in the graph, approximately 3×10^{13} copies of the associated oligonucleotide were added to the ligation reaction. Hence it is likely that many DNA molecules encoding the Hamiltonian path were created. In theory, the creation of a single such molecule would be sufficient. As a result, for this graph quantities of oligonucleotides less than an attomole would probably have been sufficient. Alternatively, a much larger graph could have been processed with the picomole quantities used here.

To implement Step 2 of the algorithm, the product of Step 1 was amplified by polymerase chain reaction (PCR) using primers O_0 and $\overline{O}_6$ (5). Thus, only those molecules encoding paths that begin with vertex 0 and end with vertex 6 were amplified. To implement Step 3 of the algorithm, the product of Step 2 was run on an agarose

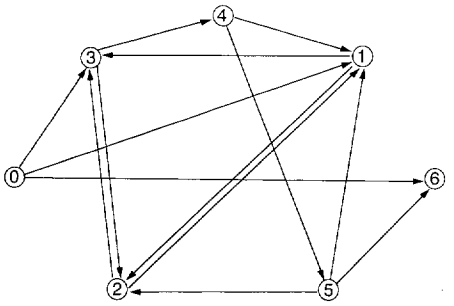

Fig. 1. Directed graph. When $v_{in} = 0$ and $v_{out} = 6$, a unique Hamiltonian path exists: 0→1, 1→2, 2→3, 3→4, 4→5, 5→6.

gel, and the 140–base pair (bp) band (corresponding to double-stranded DNA encoding paths entering exactly seven vertices) was excised and soaked in doubly distilled H_2O (ddH_2O) to extract DNA (6). This product was PCR-amplified and gel-purified several times to enhance its purity.

To implement Step 4 of the algorithm, the product of Step 3 was affinity-purified with a biotin-avidin magnetic beads system. This was accomplished by first generating single-stranded DNA from the double-stranded DNA product of Step 3 and then incubating the single-stranded DNA with $\overline{O}_1$ conjugated to magnetic beads (7). Only those single-stranded DNA molecules that contained the sequence O_1 (and hence encoded paths that entered vertex 1 at least once) annealed to the bound $\overline{O}_1$ and were retained. This process was repeated successively with $\overline{O}_2$, $\overline{O}_3$, $\overline{O}_4$, and $\overline{O}_5$. To implement Step 5, the product of Step 4 was amplified by PCR and run on a gel.

Figure 3 shows the results of these procedures. In Fig. 3A, lane 1 is the result of the ligation reaction in Step 1. The smear with striations is consistent with the construction of molecules encoding random paths through the graph (8). Lanes 2 through 5 show the results of the PCR reaction in Step 2. The dominant bands correspond to the amplification of molecules encoding paths that begin at vertex 0 and end at vertex 6.

Figure 3B shows the results of a "graduated PCR" performed on the single-stranded DNA molecules generated from the band excised in Step 3. Graduated PCR is a method for "printing" results and is performed by running six different PCR reactions with the use of O_0 as the right primer and $\overline{O}_i$ as the left primer in the ith tube. For example, on the molecules encoding the Hamiltonian path 0→1, 1→2, 2→3, 3→4, 4→5, 5→6, graduated PCR will produce bands of 40, 60, 80, 100, 120, and 140 bp in successive lanes. On the molecules encoding the path 0→1, 1→3, 3→4, 4→5, 5→6, graduated PCR will produce bands of 40, x, 60, 80, 100, and 120 bp in successive lanes, where x denotes the

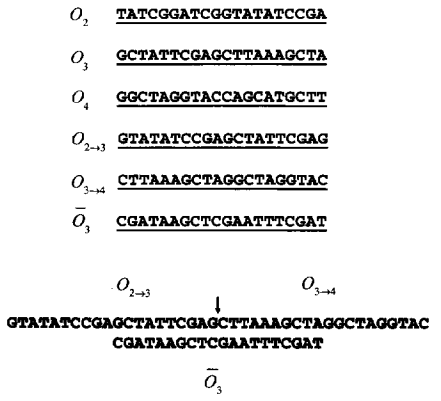

Fig. 2. Encoding a graph in DNA. For each vertex i in the graph, a random 20-mer oligonucleotide O_i is generated (shown are O_2, O_3, and O_4, for vertices 2, 3, and 4, respectively). For edge $i \rightarrow j$ in the graph, an oligonucleotide $O_{i \rightarrow j}$ is derived from the 3′ 10-mer of O_i and from the 5′ 10-mer of O_j (shown are $O_{2 \rightarrow 3}$ for edge 2→3 and $O_{3 \rightarrow 4}$ for edge 3→4). For each vertex i in the graph, $\overline{O}_i$ is the Watson-Crick complement of O_i (shown is $\overline{O}_3$, the complement of O_3). $\overline{O}_3$ serves as a splint to bind $O_{2 \rightarrow 3}$ and $O_{3 \rightarrow 4}$ in preparation for ligation. All oligonucleotides are written 5′ to 3′, except $\overline{O}_3$.

absence of a band in lane 2 (corresponding to the omission of vertex 2 along this path). On molecules encoding the path 0→3, 3→2, 2→3, 3→4, 4→5, 5→6, graduated PCR will produce bands of x, 60, 80-40, 100, 120, and 140 bp in successive lanes, where 80-40 denotes that both a 40-bp and an 80-bp band will be produced in lane 3 (corresponding to the double passage of vertex 3 along this path). The most prominent bands in Fig. 3B appear to be those that would arise from the superimposition of the bands predicted for the three paths described above. The bands corresponding to path 0→1, 1→3, 3→4, 4→5, 5→6 were not expected and suggest that the band excised in Step 3 contained contamination from 120-bp molecules. However, such low weight contamination is not a problem because it does not persist through Step 4. Figure 3C shows the results of graduated PCR applied to the molecules in the final product of Step 4. These bands demonstrate that these molecules encode the Hamiltonian path 0→1, 1→2, 2→3, 3→4, 4→5, 5→6 (9).

This computation required approximately 7 days of lab work. Step 4 (magnetic bead separation) was the most labor-intensive, requiring a full day at the bench. In general, with use of the algorithm above the number of procedures required should grow linearly with the number of vertices in the graph. The labor required for large graphs might be reduced with use of alternative procedures, automation, or less labor-intensive molecular algorithms.

The number of different oligonucleotides required should grow linearly with the number of edges. The quantity of each oligonu-

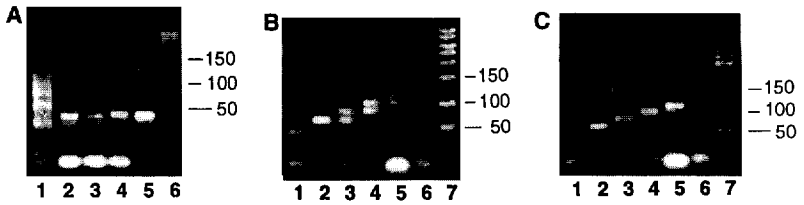

Fig. 3. Agarose gel electrophoresis of various products of the experiment. (**A**) Product of the ligation reaction (lane 1), PCR amplification of the product of the ligation reaction (lanes 2 through 5), and molecular weight marker in base pairs (lane 6). (**B**) Graduated PCR of the product from Step 3 (lanes 1 through 6); the molecular weight marker is in lane 7. (**C**) Graduated PCR of the final product of the experiment, revealing the Hamiltonian path (lanes 1 through 6); the molecular weight marker is in lane 7.

cleotide needed is a rather subtle graph theoretic question (8). Roughly, the quantity used should be just sufficient to insure that during the ligation step (Step 1) a molecule encoding a Hamiltonian path will be formed with high probability if such a path exists in the graph. This quantity should grow exponentially with the number of vertices in the graph. The molecular algorithm used here was rather naïve and inefficient, and as with classical computation, finding improved algorithms will extend the applicability of the method.

As the computation is scaled up, the possibility of errors will need to be looked at carefully. During Step 1, the occasional ligation of incompatible edge oligonucleotides may result in the formation of molecules encoding "pseudopaths" that do not actually occur in the graph. Although such molecules may be amplified during Step 2 and persist through Step 3, they seem unlikely to survive the separation in Step 4. Nonetheless, at the completion of a computation, it would be prudent to confirm that a putative Hamiltonian path actually occurs in the graph. During the separation step, molecules encoding Hamiltonian paths may fail to bind adequately and be lost, whereas molecules encoding non-Hamiltonian paths may bind nonspecifically and be retained. The latter problem might be mitigated by more stringent or repeated separation procedures. One might deal with the former problem by periodically applying PCR with primers designed to amplify Hamiltonian paths (in the example above, primers O_0 and $\overline{O}_6$). The balanced use of these techniques may be adequate to control such errors.

The choice of random 20-mer oligonucleotides for encoding the graph was based on the following rationale. First, because 4^{20} 20-mer oligonucleotides exist, choosing randomly made it unlikely that oligonucleotides associated with different vertices would share long common subsequences that might result in "unintended" binding during the ligation step (Step 1). Second, it was guessed that with high probability potentially deleterious (and presumably rare) features such as severe hairpin loops would not be likely to arise. Finally, choosing 20-mers assured that binding between "splint" and "edge" oligonucleotides would involve 10 nucleotide pairs and would consequently be stable at room temperature. This approach was successful for the small graph considered above; however, how to best proceed for larger graphs may require additional research.

What is the power of this method of computation? It is premature to give definitive answers; however, some remarks seem in order. A typical desktop computer can execute approximately 10^6 operations per second. The fastest supercomputers currently available can execute approximately 10^{12} operations per second. If the ligation (concatenation) of two DNA molecules is considered as a single operation and if it is assumed that about half of the approximately 4×10^{14} edge oligonucleotides in Step 1 were ligated, then during Step 1 approximately 10^{14} operations were executed. Clearly, this step could be scaled-up considerably, and 10^{20} or more operations seems entirely plausible (for example, by using micromole rather than picomole quantities). At this scale, the number of operations per second during the ligation step would exceed that of current supercomputers by more than a thousandfold. Furthermore, hydrolysis of a single molecule of adenosine triphosphate to adenosine monophosphate plus pyrophosphate provides the Gibbs free energy ($\Delta G = -8$ kcal mol^{-1}) for one ligation operation (*10*, *11*); hence in principle 1 J is sufficient for approximately 2×10^{19} such operations.

This is remarkable energy efficiency, considering that the second law of thermodynamics dictates a theoretical maximum of 34×10^{19} (irreversible) operations per joule (at 300 K) (*12*, *13*). Existing supercomputers are far less energy-efficient, executing at most 10^9 operations per joule. The energy consumed during other parts of the molecular computation, such as oligonucleotide synthesis and PCR, should also be small in comparison to that consumed by current supercomputers. Finally, storing information in molecules of DNA allows for an information density of approximately 1 bit per cubic nanometer, a dramatic improvement over existing storage media such as videotapes, which store information at a density of approximately 1 bit per 10^{12} nm^3.

Thus, the potential of molecular computation is impressive. What is not clear is whether such massive numbers of inexpensive operations can be productively used to solve real computational problems. One major advantage of electronic computers is the variety of operations they provide and the flexibility with which these operations can be applied. Whereas two 100-digit integers can be multiplied quite efficiently on an electronic computer, it would be a daunting task to do such a calculation on a molecular computer using currently available protocols and enzymes (*14*).

Nonetheless, for certain intrinsically complex problems, such as the directed Hamiltonian path problem where existing electronic computers are very inefficient and where massively parallel searches can be organized to take advantage of the operations that molecular biology currently provides, it is conceivable that molecular computation might compete with electronic computation in the near term. It is a research problem of considerable interest to elucidate the kinds of algorithms that are possible with the use of molecular methods and the kinds of problems that these algorithms can efficiently solve (*12*, *15*, *16*).

For the long term, one can only speculate about the prospects for molecular computation. It seems likely that a single molecule of DNA can be used to encode the "instantaneous description" of a Turing machine (*17*) and that currently available protocols and enzymes could (at least under idealized conditions) be used to induce successive sequence modifications, which would correspond to the execution of the machine. In the future, research in molecular biology may provide improved techniques for manipulating macromolecules. Research in chemistry may allow for the development of synthetic designer enzymes. One can imagine the eventual emergence of a general purpose computer consisting of nothing more than a single macromolecule conjugated to a ribosomelike collection of enzymes that act on it.

REFERENCES AND NOTES

1. R. P. Feynman, in *Minaturization*, D. H. Gilbert, Ed. (Reinhold, New York, 1961), pp. 282–296.
2. M. R. Garey and D. S. Johnson, *Computers and Intractability* (Freeman, San Francisco, CA, 1979).
3. R. M. Karp, in *Complexity of Computer Computations*, R. E. Miller and J. W. Thatcher, Eds. (Plenum, New York, 1972), pp. 85–103.
4. Each oligonucleotide (50 pmol) with 5′-terminal phosphate residue, 5 units of T4 DNA ligase (Boehringer-Mannheim, Germany), ligase buffer, and ddH_2O to a total volume of 100 μl was incubated for 4 hours at room temperature.
5. All PCR amplifications were performed on a Perkin-Elmer (Norwalk, CT) 9600 thermal cycler. For amplification in Step 2, 50 pmol of each primer and 5 units of Taq DNA polymerase (Gibco-BRL, Grand Island, NY) in PCR buffer to a total volume of 50 μl were processed for 35 cycles at 94°C for 15 s and at 30°C for

60 s. For graduated PCR, 50 pmol of each primer and 2.5 units of Taq DNA polymerase in PCR buffer to a total volume of 50 μl were processed for 25 cycles at 94°C for 15 s and at 40°C for 60 s.

6. All gels were 3 or 5% agarose (NuSieve, FMC BioProducts, Rockland, ME) in tris-borate-EDTA buffer with ethidium bromide staining (*14*).
7. Oligonucleotides were 5′ biotinylated with LC Biotin-ON Phosphoramidite (Clontech). To obtain single-stranded DNA, the product from Step 3 was amplified by PCR with the use of primers O_0 and biotinylated $\bar{O}_6$. The amplified product was annealed to streptavidin paramagnetic particles (Promega, Madison, WI) by incubating in 100 μl of 0.5× saline sodium citrate (SSC) for 45 min at room temperature with constant shaking. Particles were washed three times in 200 μl of 0.5× SSC and then heated to 80°C in 100 μl of ddH_2O for 5 min to denature the bound double-stranded DNA. The aqueous phase with single-stranded DNA was retained. For affinity purification, 1 nmol of biotinylated $\bar{O}_1$ was annealed to particles as above and washed three times in 400 μl of 0.5× SSC. Single-stranded DNA was then incubated with these particles in 150 μl of 0.5× SSC for 45 min at room temperature with constant shaking. Particles were washed four times in 400 μl of 0.5× SSC to remove unbound single-stranded DNA and then heated to 80°C in 100 μl of ddH_2O for 5 min to release single-stranded DNA bound to $\bar{O}_1$. The aqueous phase with single-stranded DNA was retained. This process was then repeated for $\bar{O}_2$, $\bar{O}_3$, $\bar{O}_4$, and $\bar{O}_5$.
8. From a graph theoretic point of view, the use of equal quantities of each oligonucleotide in the ligation reaction is not optimal and leads to the formation of large amounts of molecules encoding paths that do not start at vertex 0 nor end at vertex 6. A better way to proceed is to first calculate a flow on the graph and to use the results to determine the quantity of each oligonucleotide that is necessary.
9. On an n vertex graph G with designated vertices v_{in} and v_{out}, there may be multiple Hamiltonian paths. If it is desirable to have an explicit description of some Hamiltonian path, that can be accomplished by extending the algorithm as follows. At the end of Step 4, one has a solution (in the chemistry sense) containing molecules encoding all Hamiltonian paths for $\langle G, v_{in}, v_{out}\rangle$. The graduated PCR performed at the end of Step 4 will produce the superimposition of the bands corresponding to all of these Hamiltonian paths in the $n - 1$ successive lanes. For some lane i, a band of least weight (40 bp) will appear. This indicates that some Hamiltonian path begins with v_{in} and proceeds directly to vertex i. By amplifying by PCR the solution with primers O_i and $\bar{O}_n$, running a gel, and excising the $20 \times (n - 1)$ bp band, one can ensure that only those molecules encoding such Hamiltonian paths will be retained. One now has a solution containing molecules encoding all Hamiltonian paths for $\langle G', i, v_{out}\rangle$, where G' is the graph where vertex v_{in} has been removed. This procedure is now iterated.
10. J. D. Watson, N. H. Hopkins, J. W. Roberts, J. A. Steitz, A. M. Weiner, *Molecular Biology of the Gene* (Benjamin/Cummings, Menlo Park, CA, ed. 3, 1987).
11. M. J. Engler and C. C. Richardson, in *The Enzyme*, P. D. Boyer, Ed. (Academic Press, New York, ed. 3, 1982), vol. XVB, pp. 3–29.
12. T. D. Schneider, *J. Theor. Biol.* **148**, 125 (1991).
13. R. C. Merkle, *Nanotechnology* **4**, 21 (1993).
14. J. Sambrook, E. F. Fritsch, T. Maniatis, *Molecular Cloning* (Cold Spring Harbor Laboratory, Cold Spring Harbor, NY, ed. 2, 1989).
15. B. C. Crandall and J. Lewis, Eds., *Nanotechnology* (MIT Press, Cambridge, MA, 1992).
16. D. Bradley, *Science* **259**, 890 (1993).
17. H. Rogers Jr., *Theory of Recursive Functions and Effective Computability* (McGraw-Hill, New York, 1967).

18. The author expresses gratitude to N. Chelypov for teaching him molecular biology and thanks S. Salahuddin for making the resources of the Institute for Molecular Medicine and Technology available. The author also thanks R. Deonier for helpful discussions. Supported in part by NSF grant CCR-9214671 and a Zumberg Research Initiation Fund grant from the University of Southern California.

27 May 1994; accepted 19 September 1994

Efficient Neutralization of Primary Isolates of HIV-1 by a Recombinant Human Monoclonal Antibody

Dennis R. Burton,* Jayashree Pyati, Raju Koduri, Stephen J. Sharp, George B. Thornton, Paul W. H. I. Parren, Lynette S. W. Sawyer, R. Michael Hendry, Nancy Dunlop, Peter L. Nara, Michael Lamacchia, Eileen Garratty, E. Richard Stiehm, Yvonne J. Bryson, Yunzhen Cao, John P. Moore, David D. Ho, Carlos F. Barbas III*

The ability of antibodies to neutralize diverse primary isolates of human immunodeficiency virus–type 1 in vitro has been questioned, with implications for the likely efficacy of vaccines. A recombinant human antibody to envelope glycoprotein gp120 was generated and used to show that primary isolates are not refractory to antibody neutralization. The recombinant antibody neutralized more than 75 percent of the primary isolates tested at concentrations that could be achieved by passive immunization, for example, to interrupt maternal-fetal transmission of virus. The broad specificity and efficacy of the antibody implies the conservation of a structural feature on gp120, which could be important in vaccine design.

Protection from viral disease has traditionally been associated with the preexistence in serum of antibodies capable of neutralizing virus in vitro. Indeed, vaccines are frequently assessed on the ability to elicit neutralizing antibody responses. In the case of human immunodeficiency virus–type 1 (HIV-1), there was initial optimism about the likely efficacy of subunit vaccines given that vaccinee sera from several trials were capable of neutralizing laboratory isolates of virus in vitro (*1*, *2*). The grounds for optimism were shaken when it was found that the vaccinee sera were largely ineffective against primary isolates of HIV-1 (*2*). Some discussion subsequently centered around the validity of standard HIV-1 neutralization assays when applied to primary isolates (*2–5*). If the assays are meaningful, then they call into question the ability of antibody to effectively neutralize a spectrum of primary isolates. Hyperimmune pooled human plasma preparations are capable of neutralizing a number of primary isolates (*3–5*), but they represent a combination of specificities that might be difficult to elicit by all except the most complex vaccines (*6*). A single antibody able to effectively neutralize a broad spectrum of primary isolates would validate the vaccine approach and would provide a template for vaccine design. Furthermore, it would constitute a reagent for passive immunotherapy such as in the interruption of maternal-fetal transmission. We describe here such a human antibody derived by recombinant methods (*7*).

The generation of the antibody Fab fragment b12 from a combinatorial phage display library has been described previously (*8*). Fab b12 is directed to the CD4 binding site of gp120 and is a potent neutralizer of the HIV-1 laboratory strains IIIB and MN (*9–11*). Selection for potency and strain cross-reactivity was achieved through experimental design. The library donor was a long-term asymptomatic U.S. male, presumably infected with a clade B strain of HIV-1; the antigen for affinity selection was gp120 from the atypical IIIB strain, thereby favoring selection of cross-reactive antibodies. A large number of bacterial supernates containing antibody Fab fragments to gp120 (anti-gp120) at low initial concentrations were directly screened for neutralizing ability to find the most potent Fabs. Although Fab b12 is capable of neutralizing some primary isolates (*12*), the corresponding whole antibody molecule is likely to be more effective. Therefore, Fab b12 was converted to a whole immunoglobulin G1 (IgG1) molecule by cloning the variable region of Ig heavy chain (V_H) and light chain genes into a vector created for high-level mammalian expression (*13*). The whole antibody IgG1

D. R. Burton, P. W. H. I. Parren, C. F. Barbas III, Departments of Immunology and Molecular Biology, The Scripps Research Institute, 10666 North Torrey Pines Road, La Jolla, CA 92037, USA.
J. Pyati, R. Koduri, S. J. Sharp, G. B. Thornton, R. W. Johnson Pharmaceutical Research Institute, 3535 General Atomics Court, San Diego, CA 92121, USA.
L. S. W. Sawyer and R. M. Hendry, Viral and Rickettsial Disease Laboratory, California Department of Health Services, 2151 Berkeley Way, Berkeley, CA 94704, USA.
N. Dunlop and P. L. Nara, Laboratory of Tumor Cell Biology, Virus Biology Section, National Cancer Institute–Frederick Cancer Research and Development Center, Frederick, MD 21702, USA.
M. Lamacchia, E. Garratty, E. R. Stiehm, Y. J. Bryson, Department of Pediatrics, University of California at Los Angeles School of Medicine, 10833 Le Conte Avenue, Los Angeles, CA 90024, USA.
Y. Cao, J. P. Moore, D. D. Ho, Aaron Diamond AIDS Research Center, New York University School of Medicine, New York, NY 10016, USA.

*To whom correspondence should be addressed.